even if $|v_f| = 0$). This behavior has to do with the elastic properties of the wings, represented here by means of torsion springs of rates k. These deflect during deployment, superimposing a periodical component to the motion of the wings relative to the fuselage. Depending on the phase of this component at the time of impact, the associated impulse increases or decreases as compared with the impulse occurring with infinitely large k. Indeed, the variations in the impulse shown in Fig. 3 decrease as k increases.

Figure 4 shows $|v_{sw}|_{max}$, the maximum sidewind velocity with which deployment can still be completed, as a function of γ, and indicates that, irrespective of k, $\max(|v_{sw}|_{max})$ is obtained with $\gamma \approx 70$ deg.

The remainder of the figures are obtained with $k = 10^7$ kg-mm/rad, an unrealistically high spring rate, chosen to minimize the phenomenon implied by Fig. 3, and expose the pattern of behavior of the variables of interest. Evidently, this pattern is somewhat distorted with smaller spring rates. Thus, Figs. 5–7 show t_B and t_C, I_B and I_C, and ϕ, the roll angle, as functions of γ for $|v_{sw}|_{max} = 13$ m/s. As indicated, improvements are obtained in all of these variables, even for partial synchronization.

Finally, the following feature of the theory of imposition and relaxation of constraints, underlying the formulation of equations of motion in Ref. 1, should be pointed out, namely, that the evaluation of generalized speeds following imposition of constraints [Eqs. (42) and (43) in Ref. 1] is performed without the associated impulses having been brought into the analysis. These, however, can be evaluated at will, as in Eqs. (14) and (15). By way of contrast, conventional solutions of similar problems involve the construction of mixed equations, having both generalized speeds (at the time of impact) and impulses as unknowns. In this respect, the indicated theory is advantageous in that it suggests a methodical decoupling between equations involving the two sets of unknowns.

References

[1]Djerassi, S., and Kotzev, S., "Aircraft with Single-Axis Aerodynamically Deployed Wings," *Journal of Aircraft*, Vol. 32, No. 2, 1995, pp. 343–348.

[2]Djerassi, S., "Imposition of Constraints," *Journal of Applied Mechanics*, Vol. 61, No. 2, 1994, pp. 434–439.

Reynolds Number Effects on Vortex Breakdown of a Blunt-Edged Delta

Lance W. Traub,* Samuel F. Galls,*
and Othon K. Rediniotis†
Texas A&M University,
College Station, Texas 77843-3141

Introduction

THE breakdown of leading-edge vortices over slender delta wings is a phenomenon that has received considerable attention.[1–4] Vortex breakdown (VBD) is associated with an abrupt change in the properties of the vortex. The effect of breakdown on lift is moderate, although it does increase with wing leading-edge sweep[1] angle. VBD also degrades longitudinal stability, and introduces periodic flow structures into the wake that can cause premature fatigue of aft surfaces. Breakdown is usually associated with the core axial to rotational velocity ratio reaching a threshold, such that there is effectively insufficient axial flow to convect the axial vorticity downstream. Wing planform has a significant effect on VBD, with breakdown being delayed as leading-edge sweep increases. Straka and Hemsch[2] showed that wings with similar slenderness ratios have similar breakdown characteristics of the leading-edge vortex at the wing's trailing edge. However, once the breakdown location has moved forward of the trailing edge, the particulars of the planform have more impact. The wing's leading-edge profile is also significant, with a blunt leading edge delaying breakdown and its progression.[3] For a sharp leading edge, the form of the beveling, i.e., symmetrical or sharp edge windward or leeward, also affects VBD characteristics.[3] The leading-edge shape, and especially that at the apex, is the major reason for the discrepancy in results of different researchers testing essentially the same configuration. Straka and Hemsch[4] demonstrated that the effect of a fuselage on the location of vortex breakdown was to significantly decrease the α at which it occurred. This effect is because of the fuselage upwash effectively increasing the leading-edge camber of the wing.[5]

Most of the investigations cited previously used models with sharp leading edges, reducing sensitivity to Reynolds number. Leading-edge separation on slender blunt-edged wings is sensitive to Reynolds number, with crossflow separation being delayed by increasing Reynolds number. It is probable that breakdown for this configuration may also be Reynolds number dependent. In this Note, an experimental investigation is described that identifies the effect of a modest Reynolds number range on VBD on a blunt-edged delta wing with a fuselage.

Experimental Equipment

Model dimensions and geometry are shown in Fig. 1. The model was manufactured from Plexiglas®. The wing had a

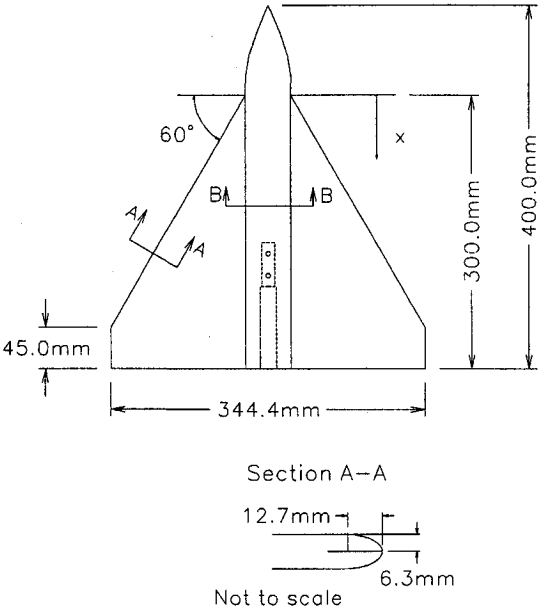

Fig. 1 Model geometry.

Received Nov. 29, 1995; revision received March 26, 1996; accepted for publication March 26, 1996.

*Graduate Student, Aerospace Engineering Department. Associate Member AIAA.

†Assistant Professor, Aerospace Engineering Department. Member AIAA.

leading-edge sweep angle of 60 deg, and was cropped slightly. The trailing edge was beveled. The wings' leading-edge profile was that of an ellipse, with a 2:1 axes ratio.

The experimental investigation was performed in the 2 by 3 ft water tunnel of the Aerospace Engineering Department of Texas A&M University. To evaluate the effects of Reynolds number, tests were run at velocities of 0.2, 0.4, and 0.6 m/s, yielding Reynolds numbers of 6.8×10^4, 13.6×10^4, and 20.3×10^4 based on the wing root chord, respectively. Selection of the point at which VBD occurs is subjective, with different researchers using different criteria. In the present study the location of breakdown was taken as the location at which the front of the core stagnation bubble was observed. It was found that for the present study, bubble-type breakdown prevailed over spiral. To aid in observation of the burst position, distance markers were drawn on the upper wing surface, which combined with observations during the test and video footage, allowed estimation of burst position. Separation of the flow at the leading edge of the wing was identified visually using dye. The location of separation was taken as the position at which injected dye no longer conformed to the wing's leading edge, but separated.

Results

Figure 2 presents the variation of breakdown position with α. It may be seen that for an angle of attack less than approximately 22 deg, VBD location is insensitive to the *Re* number range investigated. Beyond this α, increasing *Re* number is seen to delay the progression of breakdown to the apex. To ascertain the effect of leading-edge roughness on VBD, 120 grit was applied to the leading edge. As may be seen in Fig. 2, the effect is one of inducing earlier breakdown. Note the kink in the data between α = 25–30 deg, which will be detailed later.

Figure 3 shows the progression of leading-edge separation with increasing incidence. The plot shows that once separation occurs at the chordwise location of the wingtip, i.e., $x/c = 0.85$, it progresses rapidly to the $0.2x/c$ location, taking about 6 deg α, and then asymptotes to the apex. Also included in the figure are data from Rao and Johnson[6] for a similar blunt-edged delta, but with no fuselage. The lack of a fuselage may account for the discrepancy between the results. The form of the curves is seen to be similar. The aforementioned kink as seen in Fig. 2 is evident between 25–30 deg. As shown in Fig. 3, this region corresponds to an increase in the rate of progression of the point of separation, thus suggesting that as the rate of separation increases, the advancement of VBD is delayed (see Fig. 2). At approximately 15.5 deg, the position of separation stabilizes (Fig. 3), which is seen to correspond to the initial onset of VBD over the wing as shown in Fig. 2. Thus, while the point of leading edge separation is moving rapidly, VBD does not occur. Comparison of the results in Figs. 2 and 3 suggests that the tested Reynolds number range has only a marginal effect on VBD, as long as the location of leading-edge separation is not too close to the wing fuselage junction (this was shown by flow visualization).

In comparing data from the present study with that of other researchers, it is necessary to estimate the effect of the fuselage. It was assumed that the difference in the α required for leading-edge separation at a given x/c between the present data and that of Rao and Johnson[6] may be attributed to fuselage effects. This difference in α at each corresponding x/c location was subtracted from the results of Erickson[7] for a sharp-edged 60-deg delta with no fuselage, and the result is shown in Fig. 4. Also included is a correction to Erickson's results to account for the fuselage based upon that suggested by Straka and Hemsch.[4] The correlation between the results of Erickson modified to simulate the presence of the fuselage using the two methods described earlier is seen to be good for $(x/c)_{VBD} > 0.6$. It may be seen in Fig. 4 that the effect of a blunt leading edge is generally one of delaying VBD. For $(x/c)_{VBD} < 0.5$ break-

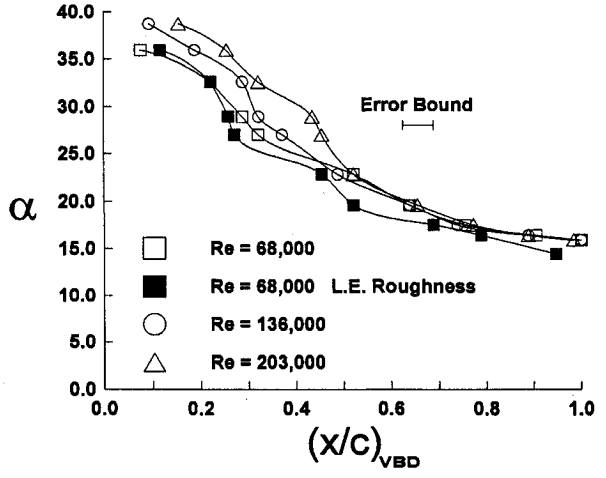

Fig. 2 Effect of Reynolds number on vortex burst trajectory.

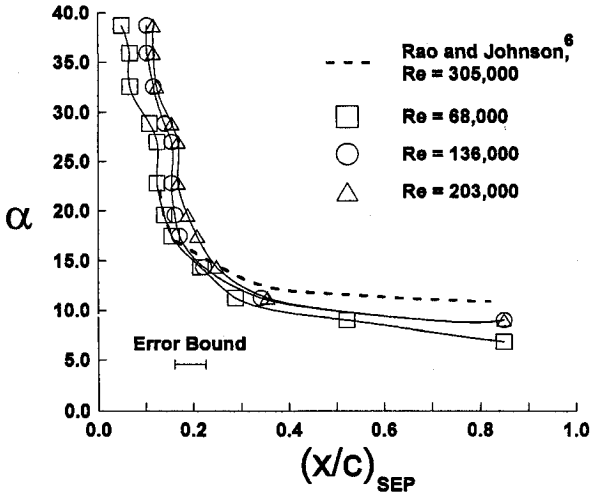

Fig. 3 Effect of Reynolds number on leading-edge separation.

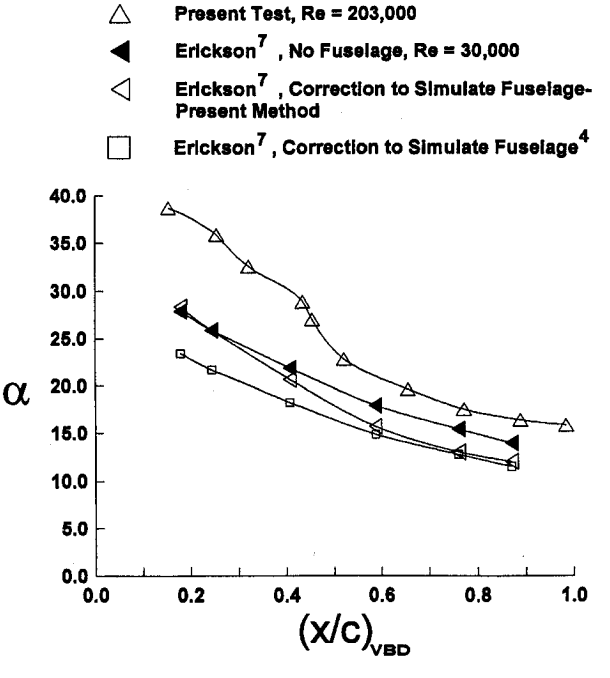

Fig. 4 Effect of sharp and blunt leading edge on vortex burst trajectory.

down is shown to be delayed substantially compared to the sharp-edged wing.

Concluding Remarks

It has been shown that for the model tested in this study, Reynolds number effects are only manifested when the rate of progression of the location of leading-edge crossflow separation has slowed, which typically occurs when the separation region is close to the wing/fuselage junction. Vortex breakdown was not observed while leading-edge flow separation was progressing rapidly from the wing trailing edge to the apex. The blunt leading edge was seen to significantly delay vortex breakdown compared to a comparative sharp-edged wing.

Acknowledgment

The authors would like to thank Conrad Wilson for the skilled manufacture of the test model.

References

[1]Wentz, W. H., and Kohlman, D. L., "Vortex Breakdown on Slender Sharp-Edged Wings," *Journal of Aircraft*, Vol. 8, No. 3, 1971, pp. 156–161.

[2]Straka, W. A., and Hemsch, M. J., "Leading-Edge Vortex Breakdown for Wing Planforms with the Same Slenderness Ratio," *Journal of Aircraft*, Vol. 31, No. 3, 1994, pp. 688–695.

[3]Kegelman, J. T., and Roos, F. W., "Effects of Leading-Edge Shape and Vortex Burst on the Flowfield of a 70-Degree-Sweep Delta Wing," AIAA Paper 89-0086, Jan. 1989.

[4]Straka, W. A., and Hemsch, M. J., "Effect of a Fuselage on Delta Wing Vortex Breakdown," *Journal of Aircraft*, Vol. 31, No. 4, 1994, pp. 1002–1005.

[5]Ericcson, L. E., "Comment on Effect of a Fuselage on Delta Wing Vortex Breakdown," *Journal of Aircraft*, Vol. 31, No. 4, 1994, pp. 1006, 1007.

[6]Rao, D. M., and Johnson, T. D., Jr., "Alleviation of the Subsonic Pitch-Up of Delta Wings," *Journal of Aircraft*, Vol. 20, No. 6, 1983, pp. 530–535.

[7]Erickson, G. E., "Flow Studies of Slender Wing Vortices," AIAA Paper 80-1423, July 1980.

Ring Wing for a Compressed Missile

Henry August* and Frederick W. Hardy†
Hughes Missile Systems Company,
Tucson, Arizona 85706
and
Russell Osborn† and Mark Pinney‡
U.S. Air Force Wright Laboratory,
Wright–Patterson Air Force Base, Ohio 45433

Introduction

TO enhance weapon/aircraft system survivability and mission success, future aircraft require advanced air-to-ground and air-to-air weapons that minimally contribute to the drag and observable characteristics of the integrated weapon system. Evaluation of potential ring wing missile applications have focused on providing a technology base from which effective low installed drag and low observable weapon/aircraft integration designs and techniques can evolve for current and future aircraft. Compared to conventional planar wings, a ring wing having equal planform area generates higher lift and greater aerodynamic efficiency (lift-to-drag ratio). By providing a physical barrier at its wingtips, spillage of high-pressure air from the lower to the upper surface of the ring wing is constrained. In this manner, typical wingtip losses are avoided. Consequently, a ring wing missile can achieve improved free-flight performance including extended range and cross range as well as provide greater maneuverability.

Extendable Ring Wing Concept

A unique design of an extendable ring wing provides configuration flexibility while in flight that is tailored to its mission.[1] During its compressed carriage on an aircraft, the wing is wrapped around the missile's body and subsequently unfurls during the missile's free flight (Fig. 1).

Extendable wraparound tail surfaces can similarly be used. In its compact version, the missile is bullet-like in shape with minimal size and volume. A compressed ring wing missile can be carried externally by an aircraft with reduced installed drag and lowered radar reflectivity.[2] Also, many more missiles can be carried within a given-sized bay of an aircraft. In addition, a compressed ring wing missile is conducive to rearward tube-launching techniques from underwing conformal pods.

These unique features of a ring wing missile can favor a pilot with increased flexibility in his flight approach to a defended ground target. In this manner, he and his aircraft can enjoy enhanced survivability as well as enhance the success of his mission.

Compressed Weapons

By providing compressed weapon designs for internal and external carriage installations on LO aircraft, weapon loadouts, and strike force capabilities can be maximized. A ring wing flexible band design and wraparound tail surfaces have been functionally demonstrated at low speeds and are inherently suitable for achieving compressed volume compared to a conventional wing round body missile. Upon launch of the missile, ring wing extendable lifting surfaces are mechanized to deploy and provide self-extension and locking (Fig. 2).

Ring Wing Deployment Mechanisms

A flexible band ring wing was constructed from flat spring-like sheet material (aluminum; 0.040 in. thickness) and force-wrapped one circumference around the missile body's circular section in a wingtip-to-wingtip fashion. This activates resistive bending stresses within the flexible outer band structure of the ring wing, which tends to restore the panel to its planar shape. In this manner, the activation energy for ring wing deployment is supplied. To constrain the ring wing from opening inadvertently, a mechanical locking/release device is applied across adjacent wingtips. Such a device has been successfully employed during wind-tunnel demonstrations of ring wing deployment[1] on a full-scale ring wing missile test model (13.5-in. body diameter) representative of a typical air-to-ground weapon (Fig. 3). A flat metallic, holdback disk supported on a stem attached to the missile model's inner structure was used. This disk constrained the movement of the adjacent wingtip edges of the ring wing by forcing them against the missile body. Using pneumatic actuation, the disk was displaced radially away from the missile's body. This permitted the wingtips to clear the holdback disk thereby allowing the ring wing's flexible outer band to unfurl and extend. On reaching full extension, wing panel hinges were locked by square-shaped, spring-activated, axial pins. Full deployment was achieved in about 0.2 s. In low-speed airflow, similar demonstrations were made at angles of attack of +10 deg. Under these conditions,

Received April 17, 1995; revision received Dec. 20, 1995; accepted for publication Feb. 20, 1996.

*Laboratory Scientist. Associate Fellow AIAA.

†Technical Manager.

‡Senior Aerospace Engineer.